AMERICAN SOCIETY FOR MICROBIOLOGY | Antimicrobial Agents and Chemotherapy®

ANTIVIRAL AGENTS

A New Role for Capsid Assembly Modulators To Target Mature Hepatitis B Virus Capsids and Prevent Virus Infection

Chunkyu Ko,[a] Romina Bester,[a] Xue Zhou,[b] Zhiheng Xu,[b] Christoph Blossey,[a] Julia Sacherl,[a] Florian W. R. Vondran,[c,d] Lu Gao,[b] Ulrike Protzer[a,e]

[a]Institute of Virology, Technical University of Munich/Helmholtz Zentrum München, Munich, Germany
[b]Roche Innovation Center Shanghai, Shanghai, China
[c]ReMediES, Department of General, Visceral and Transplant Surgery, Hannover Medical School, Hannover, Germany
[d]German Centre for Infection Research (DZIF), Partner Site Hannover-Braunschweig, Hannover, Germany
[e]German Center for Infection Research (DZIF), Munich Partner Site, Munich, Germany

ABSTRACT Hepatitis B virus (HBV) is a major human pathogen, killing an estimated 887,000 people per year. Therefore, potentially curative therapies are of high importance. Following infection, HBV deposits a covalently closed circular DNA (cccDNA) in the nucleus of infected cells that serves as a transcription template and is not affected by current therapies. HBV core protein allosteric modulators (CpAMs) prevent correct capsid assembly but may also affect early stages of HBV infection. In this study, we aimed to determine the antiviral efficacy of a novel, structurally distinct heteroaryldihydropyrimidine (HAP)-type CpAM, HAP_R01, and investigated whether and how HAP_R01 prevents the establishment of HBV infection. HAP_R01 shows a significant inhibition of cccDNA formation when applied during the first 48 h of HBV infection. Inhibiting cccDNA formation, however, requires >1-$\log_{10}$-higher concentrations than inhibition of the assembly of newly forming capsids (half-maximal effective concentration [EC_{50}], 345 to 918 nM versus 26.8 to 43.5 nM, respectively). Biophysical studies using a new method to detect the incoming capsid in *de novo* infection revealed that HAP_R01 can physically change mature capsids of incoming virus particles and affect particle integrity. Treating purified HBV virions with HAP_R01 reduced their infectivity, highlighting the unique antiviral activity of CpAMs to target the capsid within mature HBV particles. Accordingly, HAP_R01 shows an additive antiviral effect in limiting *de novo* infection when combined with viral entry inhibitors. In summary, HAP_R01 perturbs capsid integrity of incoming virus particles and reduces their infectivity and thus inhibits cccDNA formation in addition to preventing HBV capsid assembly.

KEYWORDS antiviral agents, capsid, core protein, core protein allosteric modulators, covalently closed circular DNA, hepatitis B virus

Hepatitis B virus (HBV) infection is a global health problem with 257 million chronic carriers worldwide who are at a high risk of developing liver diseases such as liver cirrhosis and hepatocellular carcinoma (1). Although new infections and mother-to-child transmission can be controlled by hepatitis B vaccine, hepatitis B immunoglobulin (HBIG), and potent antivirals, hepatitis B surface antigen (HBsAg) seroprevalence is estimated at over 8% in areas of high endemicity, especially in sub-Saharan Africa and in Asia (2). Curative treatment options for individuals already infected with HBV are still lacking. Current treatment of chronic hepatitis B includes orally administered nucleos(t)ide analogues (NUCs), such as entecavir (ETV) and tenofovir (TDF), which inhibit the reverse transcriptase activity of HBV polymerase, and subcutaneously administered interferons. NUCs efficiently suppress virus replication, have an excellent safety profile,

Citation Ko C, Bester R, Zhou X, Xu Z, Blossey C, Sacherl J, Vondran FWR, Gao L, Protzer U. 2020. A new role for capsid assembly modulators to target mature hepatitis B virus capsids and prevent virus infection. Antimicrob Agents Chemother 64:e01440-19. https://doi.org/10.1128/AAC.01440-19.

Address correspondence to Ulrike Protzer, protzer@tum.de.

Received 21 July 2019
Returned for modification 8 August 2019
Accepted 18 October 2019
Accepted manuscript posted online 28 October 2019
Published 20 December 2019

and can reduce the risk of liver disease and mortality. However, NUCs cannot eliminate episomal covalently closed circular DNA (cccDNA) that serves as the template for viral transcription and represents the viral persistence form (3). Thus, there is a high need to develop new and potentially curative therapeutic approaches that target cccDNA.

HBV is a small enveloped virus containing partially double-stranded, relaxed circular DNA (rcDNA) within its capsid (4). The icosahedral HBV capsid spontaneously assembles from 120 dimers of HBV core protein. HBV core protein and its assembled capsid play a role in virtually every step of the HBV life cycle. During cell entry, the incoming particle releases the capsid that delivers the HBV rcDNA genome into the nucleus, where rcDNA is converted into cccDNA. Core protein associates with cccDNA and is implicated in epigenetic regulation of cccDNA (5). Later in infection, viral DNA synthesis occurs within newly assembled capsids via reverse transcription of a pregenomic RNA (pgRNA), giving rise to rcDNA. During formation of new viral genomes, capsids facilitate pgRNA packaging and minus-strand and plus-strand DNA synthesis rather than being inert containers (6–8). Subsequently, rcDNA-containing capsids are enveloped and released from the cells or alternatively recycled back to the nucleus to maintain or amplify cccDNA (9).

Core protein allosteric modulators (CpAMs), also called capsid assembly inhibitors, are small molecules capable of modulating capsid assembly (10). Several chemical classes of CpAMs, including phenylpropenamide (PPA), heteroaryldihydropyrimidine (HAP), and sulfamoylbenzamide (SBA), have been identified, and the first compounds are in early clinical trials (3). PPA derivative AT130 selectively prevents pgRNA packaging, resulting in empty capsids that are morphologically identical to wild-type capsids (11). HAP derivative Bay41-4109 accelerates and misdirects capsid assembly *in vitro* (12) and depletes newly synthesized core protein by reducing its half-life in cell culture (13). HAP_R01 is a novel HAP-type CpAM (Fig. 1A) that binds to the core protein dimer-dimer interface and effectively inhibits HBV replication and HBeAg biosynthesis in HBV-replicating hepatoma cells (14–16).

While studies have shown that CpAMs can inhibit cccDNA formation during *de novo* HBV infection (17–19), further mechanism-of-action (MOA) studies are needed to elucidate whether and how CpAMs target capsid of incoming virus particle and affect early stages of HBV infection. Studying this, we found that HAP_R01 inhibits cccDNA formation in primary human hepatocytes (PHH), HepaRG cells, and sodium taurocholate cotransporting polypeptide (NTCP)-reconstituted hepatoma cells (HepG2-NTCP-K7) (9) with 10- to 30-fold-reduced efficacy compared to its inhibitory effect on the formation of new virions. Mechanistic analysis demonstrated that HAP_R01 directly acts on preformed HBV capsids, resulting in aberrant core protein polymers that are depleted in infected cells. HAP_R01 was also able to target the capsids from incoming virions and reduce HBV particle infectivity. Furthermore, we showed an additive antiviral effect of HAP_R01 when combined with entry inhibitors.

RESULTS

HAP_R01 inhibits cccDNA formation. To study the effect of HAP_R01 in HBV infection, we used a highly permissive HepG2 cell clone expressing NTCP (HepG2-NTCP-K7) that is well characterized in terms of infection kinetics and cccDNA dynamics and supporting 1 to 9 copies of cccDNA per cell (9). Since HAP_R01 has been reported to prevent capsid formation (15), we focused on its effects on a preformed capsid. Considering that cccDNA formation is a slow process requiring 3 days (9), HepG2-NTCP-K7 cells were either pretreated (pre) with HAP_R01 or treated during (day 0 [d0] to -3) or after (d3 to -8) cccDNA establishment (Fig. 1B). Interestingly, cccDNA levels were significantly reduced when HAP_R01 was applied during the first 3 days when HBV infection was being established (Fig. 1B). At equal doses, Bay41-4109 and AT130 reduced cccDNA levels to a lesser extent than HAP_R01 (see Fig. S1 in the supplemental material). The inhibitory effect on cccDNA was independent of the multiplicity of infection (MOI) of HBV used (Fig. S2). In contrast, neither pretreatment, i.e., 48-h

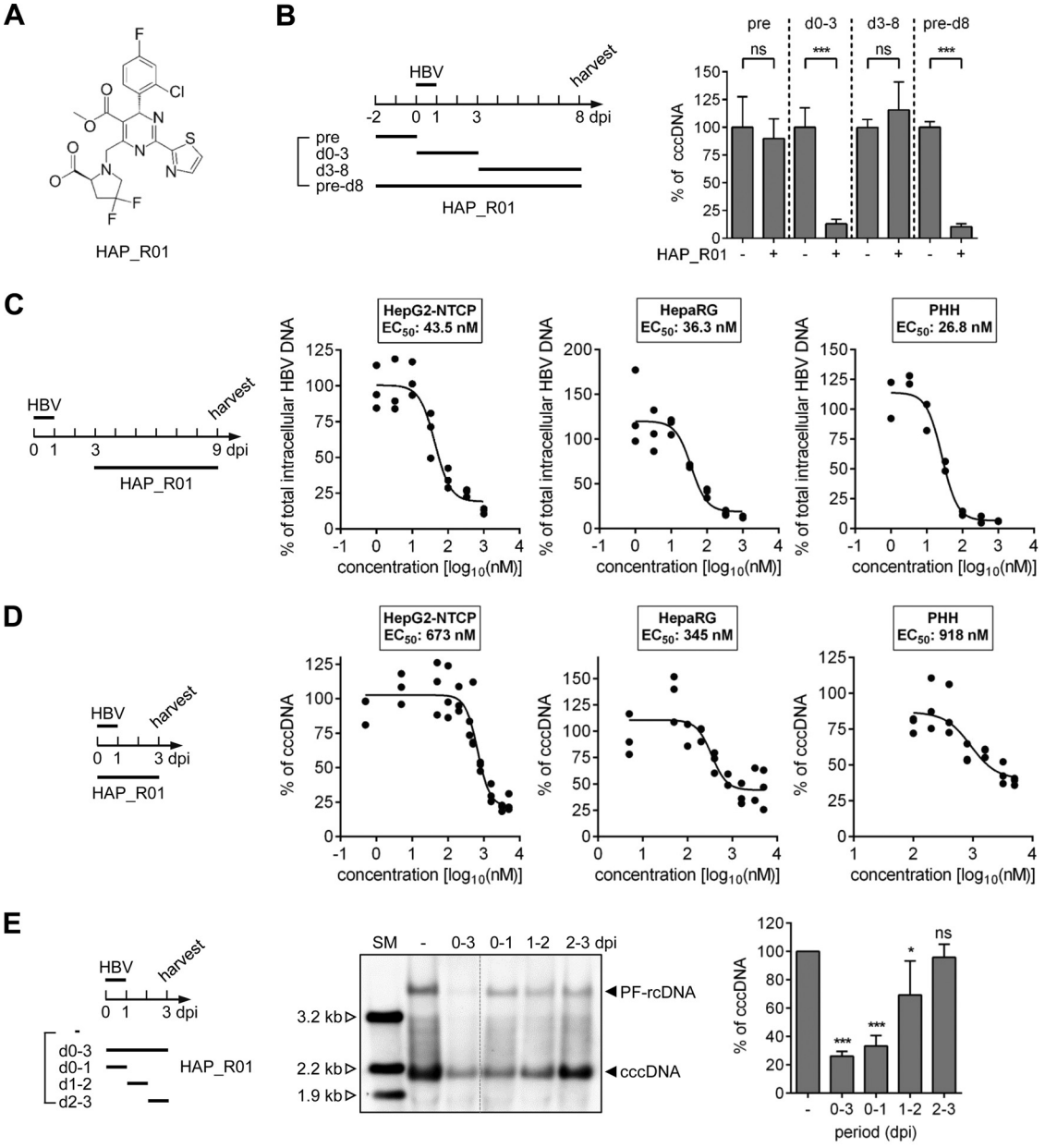

FIG 1 Evaluation of the effect of HAP_R01 on cccDNA establishment. (A) Chemical structure of HAP_R01. (B) HepG2-NTCP-K7 cells were infected with HBV at an MOI of 100 virus particles (vp)/cell and treated with 5 μM HAP_R01 at different time periods as indicated. Extracted total cellular DNA was subjected to cccDNA qPCR. (C and D) Cells were treated with increasing concentrations of HAP_R01 either from 3 days postinfection (dpi) until 9 dpi (C) or at the time of HBV inoculation for 3 days (D). Levels of intracellular HBV-DNA (C) and cccDNA (D) were analyzed by qPCR. The half-maximal effective concentration (EC_{50}) of HAP_R01 required to inhibit viral DNA production and cccDNA formation was calculated by nonlinear regression analysis after generating a dose-response curve. (E) HepG2-NTCP-K7 cells were infected with HBV at an MOI of 500 vp/cell and treated with 5 μM HAP_R01 at different time periods as indicated. DNA extracted according to the Hirt procedure was assayed by Southern blotting with an HBV-DNA probe. cccDNA and protein-free rcDNA (PF-rcDNA) are denoted. Restriction fragments of HBV-DNA (3.2 to 1.9 kb) serve as a size-marking ladder. A representative image is shown. cccDNA bands were quantified from four independent experiments and Southern blots, and the percent values of cccDNA (relative to untreated control) were plotted in a bar graph (mean $\pm$ SD; $n = 4$). Student's t test was used (***, $P \leq 0.001$; *, $P \leq 0.05$; ns, not significant).

treatment before infection (pre), nor treatment after cccDNA formation (d3 to -8) diminished cccDNA levels (Fig. 1B).

HAP_R01 inhibited new HBV-DNA production at a half-maximal effective concentration (EC_{50}) ranging from 26.8 to 43.5 nM depending on cell type (Fig. 1C). However, 10- to 30-fold-higher concentrations were needed to inhibit cccDNA formation (EC_{50},

345 to 918 nM) upon HBV infection of HepG2-NTCP-K7 cells, HepaRG cells, and primary human hepatocytes (PHH) (Fig. 1D). Without treatment, HBV-infected HepaRG cells and PHH contained 0.3 to 0.6 and 0.5 to 1 cccDNA copies/cell, respectively. HAP_R01 had no detectable cytotoxicity under the conditions examined (Fig. S3).

To delineate the time period during which HAP_R01 inhibits cccDNA formation, we performed additional time-of-addition experiments (Fig. 1E). Southern blot analysis showed that the most significant reduction in cccDNA and protein-free rcDNA was achieved by continuous HAP_R01 treatment for 3 days (d0 to -3) and, to a lesser extent, by coadministering HAP_R01 during (d0 to -1) or early after (d1 to -2) HBV infection (Fig. 1E). In contrast, HAP_R01 failed to reduce cccDNA levels after 2 days postinfection (p.i.) (Fig. 1E; d2 to -3). Secretion of HBeAg as an indirect marker of transcriptionally active intranuclear cccDNA (9) correlated with cccDNA levels (Fig. S4). Overall, these results demonstrate that HAP_R01 not only blocks formation of new virions but also inhibits the establishment of cccDNA formation, and they are consistent with previous reports showing that selected CpAMs have dual effects on the virus life cycle (17–19).

HAP_R01 alters capsid structure and integrity. Given that HAP_R01 showed an effect on establishing cccDNA only during the first 48 h p.i. (Fig. 1E), the most likely target was the incoming HBV capsid. To investigate whether HAP_R01 can destabilize preformed capsids, we treated purified recombinant HBV capsids composed of C-terminally truncated core proteins (amino acids 1 to 149) with HAP_R01 and investigated structural alterations by electron microscopy. As shown in Fig. 2A, HAP_R01 transformed 35-nm capsids into irregular core protein structures of >100-nm size, showing a direct effect of HAP_R01 on capsids.

Since *Escherichia coli*-expressed HBV capsids do not contain HBV genomes, biochemical and structural properties differ from those of mature, infectious capsids that contain rcDNA (20). Thus, we established a method to isolate and analyze mature capsids from hepatoma cells constitutively expressing the large HBV envelope protein (L-HBsAg)-deficient but replication-competent HBV genomes (HepG2-NTCP-K7-H1.3L$^-$) that we have recently described (9) and accumulate intracellular capsids (Fig. S5). Three distinct populations were observed by dot blot analysis of cesium chloride (CsCl) density gradient fractions (Fig. 2B). Fractions 8 to 9 (density, 1.34 to 1.37 g/ml) contained capsids and viral nucleic acids, whereas fractions 11 to 12 (density, 1.25 to 1.28 g/ml) exclusively contained capsids. Low-density fractions 16 to 18 (density, 1.12 to 1.17 g/ml) appeared to contain core protein aggregates, as we observed a slower and diffuse migration pattern (Fig. S6). Analysis of HBV-DNA content by quantitative real-time PCR (qPCR) showed that capsids in fractions 8 to 9 had packaged viral DNA (Fig. 2B).

Native agarose gel electrophoresis confirmed the identity of two capsid populations: HBV-DNA-containing capsids (fractions 8 to 9) and empty capsids devoid of viral nucleic acids (fractions 11 to 12) (Fig. S6). No loss of HBV-DNA signal after DNase I treatment in pooled fractions 8 to 9 confirmed that HBV-DNA resides within capsids (data not shown). Southern blotting of DNA isolated from fractions 8 to 9 showed that the majority of capsids contain either rcDNA (67%) or double-stranded linear DNA (dlDNA) (16%) (Fig. 2C).

Having isolated mature capsids, we investigated if HAP_R01 would induce structural changes of the capsids that could be detected by a mobility shift in native agarose gel electrophoresis (21). Interestingly, we observed a mobility shift of capsid and HBV-DNA bands already after 1-h HAP_R01 treatment (5,000 nM) (Fig. 2D, top), suggesting an altered surface charge and shape of the capsid resulting in reduced electrophoretic mobility. Capsid mobility was not altered in ETV-, Bay41-4109-, or AT130-treated samples (Fig. 2E, top). A similar mobility shift was observed when empty capsids were incubated with HAP_R01, confirming HAP_R01-mediated capsid distortion independent of packaged viral genomes (Fig. S7). Prolonged incubation with HAP_R01 resulted in altered capsid mobility at 500 nM and, to a lesser extent, at 50 nM and with Bay41-4109 at 5,000 nM (Fig. 2D and E, bottom). Unexpectedly, we noted an increased

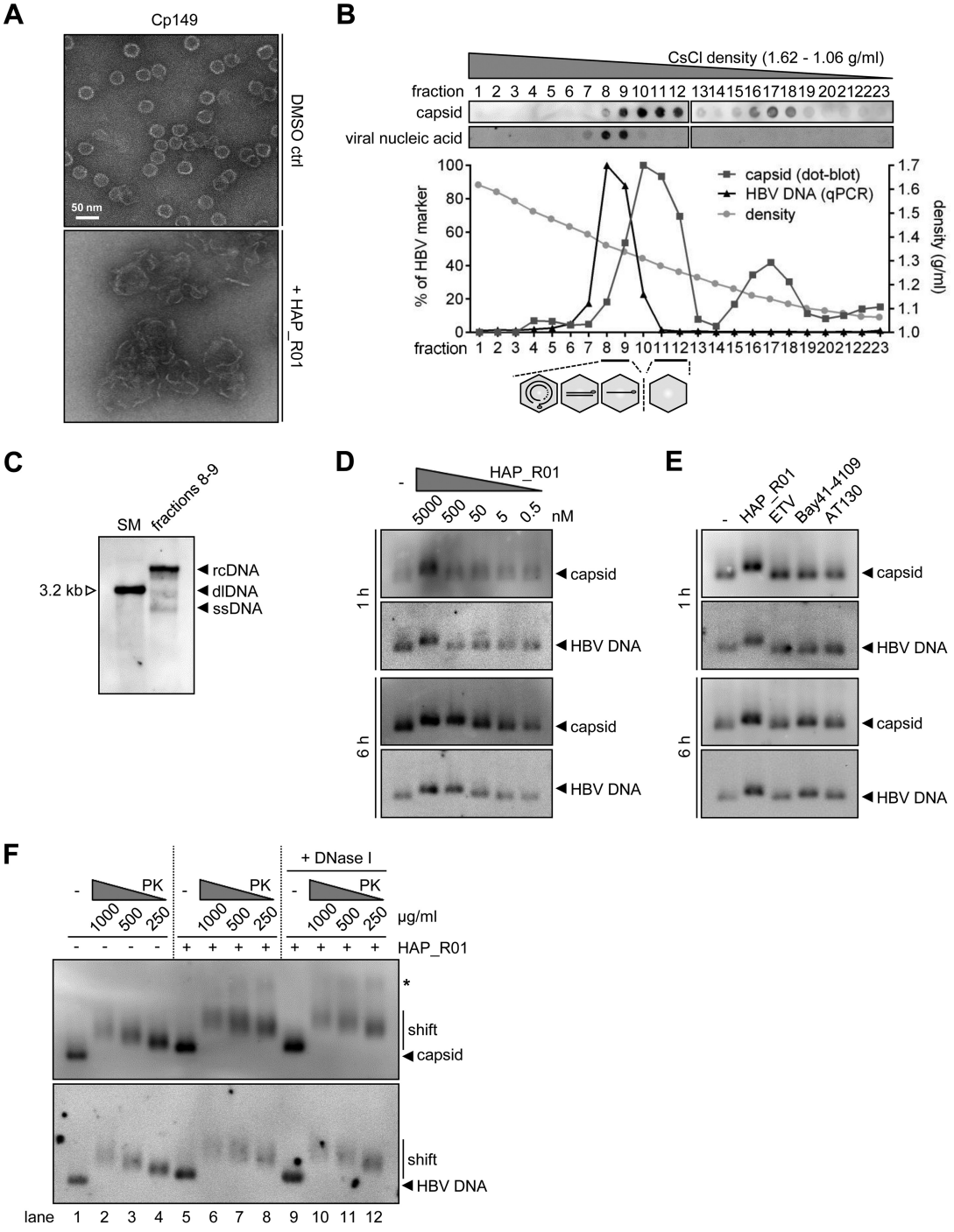

FIG 2 Effect of HAP_R01 on capsids *in vitro*. (A) Recombinant capsids purified from *E. coli* expressing C-terminally truncated form of core protein (Cp1–149) were either mock treated or treated with 20 μM HAP_R01 for 3 h in 250 mM NaCl and 50 mM HEPES (pH 7.4). Electron microscopic images of negatively stained capsids are shown. (B) Cytoplasmic lysate from HepG2-NTCP-K7-H1.3L$^-$ cells was subjected to CsCl density gradient ultracentrifugation, and 23 fractions were collected from bottom to top. Aliquots of each fraction were transferred onto a PVDF membrane by using a dot blot device, and capsid levels were analyzed by immunoblotting with an anticore antibody (Dako) which preferentially recognizes capsid rather than denatured core protein (22). Viral nucleic acids on the same membrane were subsequently detected by an HBV-DNA probe. Additionally, total cellular DNA was extracted from each fraction and analyzed by HBV-DNA qPCR. Relative amounts of capsid and total intracellular HBV-DNA in each fraction were quantified and plotted together with CsCl densities. (C) DNA was extracted from pooled fractions 8 to 9 and subjected to Southern blot analysis. rcDNA, dlDNA, and single-stranded DNA (ssDNA) are denoted together with a 3.2-kb HBV-DNA fragment serving as a size marker. (D to F) Capsid and capsid-associated HBV-DNA contents were analyzed by native agarose gel analysis in the absence of SDS (see the supplemental material). The concentration of DMSO was 1% under all conditions. Pooled fractions 8 to 9 were treated with either increasing concentrations of HAP_R01 (D) or different anti-HBV compounds (5 μM each) (E) at 37°C for 1 h and 6 h. (F) Pooled fractions 8 to 9 were either mock treated or treated with 5 μM HAP_R01 at 37°C for 1 h. Increasing concentrations of proteinase K alone or in combination with DNase I (5 U) were added for an additional 1 h.

capsid and HBV-DNA signal on the blot. This likely resulted from an increased accessibility of the altered capsids for antibody and probe binding, as the same pattern was observed using another anticore antibody (Fig. S8). These findings indicate that HAP_R01 can directly target HBV capsids and induce abnormal core-protein structures more efficiently than other CpAMs, including Bay41-4109 and AT130.

To further our understanding of HAP_R01-induced structural alterations, we analyzed the sensitivity of mature capsids to proteinase K alone or in combination with DNase I after HAP_R01 treatment (Fig. 2F). Proteinase K resulted in an enhanced mobility shift of capsid and a reduced intensity of HBV-DNA bands (Fig. 2F, lanes 6 to 8), whereas additional DNase I treatment did not affect electrophoretic mobility (Fig. 2F, lanes 10 to 12). Besides the main capsid population, a population of slow-migrating capsids (denoted with an asterisk) was detected in HAP_R01-treated cells that apparently did not contain HBV-DNA anymore (Fig. 2F, lanes 6 to 8 and 10 to 12). In summary, our *in vitro* studies using both rcDNA-containing mature capsids and *E. coli*-expressed capsids demonstrate that HAP_R01 can target, destabilize, and distort capsids, resulting in aberrant core-protein polymers.

HAP_R01 destabilizes and diminishes incoming capsids during *de novo* HBV infection. The results shown above suggested that HAP_R01 can target incoming capsids during infection and inhibit cccDNA establishment. To determine optimal conditions for the analysis of incoming capsids using the new method we have established, we performed a time course study after infection with highly purified virions (Fig. 3A). By treating cells with trypsin and subsequent NP-40 lysis, we were able to analyze the incoming, cytoplasmic capsids after virus uptake. Intracellular capsids, capsid-associated HBV-DNA, and core protein were detected starting from 1 h p.i. (Fig. 3B and C). Notably, a smear of both core protein and HBV-DNA migrating slower than capsids and capsid-associated DNA was detected (denoted with asterisks) (Fig. 3B). This smear was not shown in newly synthesized capsids (Fig. S9), indicating a certain heterogeneity of incoming capsids that does not reflect the HBV inoculum (data not shown). Quantitative analysis showed an increase of capsids over time with a maximum reached at 8 h p.i. (Fig. 3D). A gradual decrease observed after 8 h could be explained by either capsid dissociation after HBV genome release into the nucleus (22) or capsid degradation, exceeding the amount of newly entering virions.

At 5 h p.i., when most capsids entered the cells but the decay had not started yet, HAP_R01 induced a 50% reduction in cytoplasmic capsids along with a modest retardation in capsid electrophoretic mobility (Fig. 3E). In contrast, ETV had no effect on capsid levels or their mobility. Notably, a corresponding reduction in core protein levels was observed by Western blotting (Fig. S10), suggesting HAP_R01-mediated capsid depletion and degradation. Comparable results were observed when measuring levels of capsid and core protein in an independent time course experiment (Fig. 3F). Treating cell lysates with proteinase K enhanced the electrophoretic mobility shift of incoming capsids in particular after HAP_R01 treatment, while DNase had no additional effect (Fig. 3E). This strongly suggests that HAP_R01 deforms the incoming capsids but that structurally altered capsids still hold HBV-DNA. To test a possibility that large, aberrant core polymers or a trace amount of HBV-DNA released into the cytoplasm contributes to the reduced cccDNA formation upon HAP_R01 treatment, we examined the expression of interferon-stimulated genes (ISGs) at early time points after HBV infection (Fig. S11). HAP_R01 treatment during HBV inoculation for 6 and 24 h did not induce ISG expression, suggesting a negligible role of host innate immune response. Overall, our data indicate that HAP_R01 destabilizes the incoming capsid and thereby affects cccDNA establishment during *de novo* infection.

HAP_R01 targets extracellular HBV particles and reduces particle infectivity. Since HAP_R01 showed the most significant reduction in cccDNA formation when present during and up to 24 h after infection (Fig. 1E), we wondered whether HAP_R01 may target newly infecting particles. To investigate this, HBV particles were incubated with HAP_R01 or other CpAMs and recovered by centrifugal filtration prior to evaluating infectivity (Fig. 4A). Treating HBV with HAP_R01 for 8 h or longer resulted in a viral

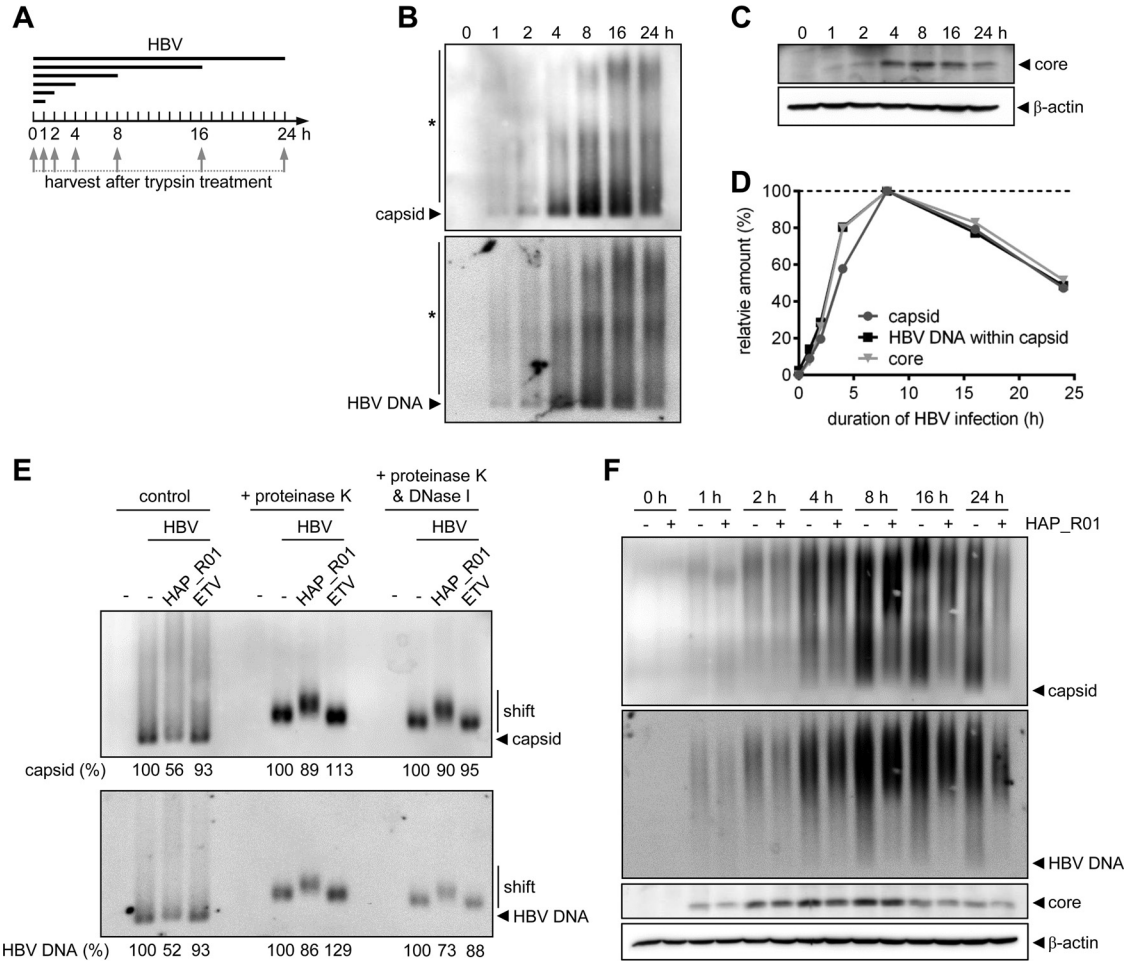

FIG 3 Effect of HAP_R01 on incoming capsids in *de novo* HBV infection. (A) HBV-infected (500 vp/cell) HepG2-NTCP-K7 cells were harvested at different time points. Before harvest, cells were treated with trypsin for 3 min to remove membrane-associated input virus particles. (B and C) Cytoplasmic capsid and capsid-associated HBV-DNA (B) and core protein (C) were detected by native agarose gel analysis and Western blot analysis, respectively. β-Actin serves as a loading control. (D) Relative amounts of capsid and HBV-DNA within the capsid and core protein were quantified and plotted with the 8-h HBV inoculation condition set to 100%. (E) HepG2-NTCP-K7 cells were either treated with PEG (mock infection) or infected with HBV at an MOI of 500 vp/cell for 5 h in the presence or absence of HAP_R01 or ETV (5 μM each). Obtained cytoplasmic lysate was either mock treated or treated with proteinase K (1 mg/ml) alone or proteinase K plus DNase I (5 U) at 37°C for 1 h. Capsid and capsid-associated HBV-DNA were analyzed and quantified relative to untreated control. (F) HepG2-NTCP-K7 cells were infected with HBV in the presence or absence of HAP_R01. Cytoplasmic capsid and core protein levels were analyzed at indicated time points. PEG, polyethylene glycol.

inoculum that established reduced levels of cccDNA (Fig. 4B), whereas preincubation with AT130 had no effect (Fig. 4C). Bay41-4109 preincubation also reduced HBV infectivity, although to a lesser extent than HAP_R01. Of note, HAP_R01 reduced the level of incoming capsid and core protein both during HBV infection, when HAP_R01 was in direct contact with HBV particles, and shortly after HBV infection, when a direct contact of HAP_R01 with the inoculum was unlikely (Fig. S12). Collectively, these results highlight a role for HAP_R01 to target both extracellular HBV particles and intracellular, incoming capsids.

HAP_R01 and entry inhibitors show additive effects on cccDNA establishment. Given that HAP_R01 can prevent *de novo* cccDNA formation by altering incoming capsid integrity and reducing HBV infectivity, we wondered if a combination of HAP_R01 with entry inhibitors or a NUC could inhibit cccDNA formation more efficiently. This would allow us to provide a rationale of potential application of CpAMs in a combination with other antiviral agents. To evaluate this, HAP_R01 was applied either alone or in combination with suboptimal doses of clinical-grade anti-HBV immunoglobulin (HBIG; Hepatect CP), the synthetic peptide Myrcludex B (MyrB) derived from

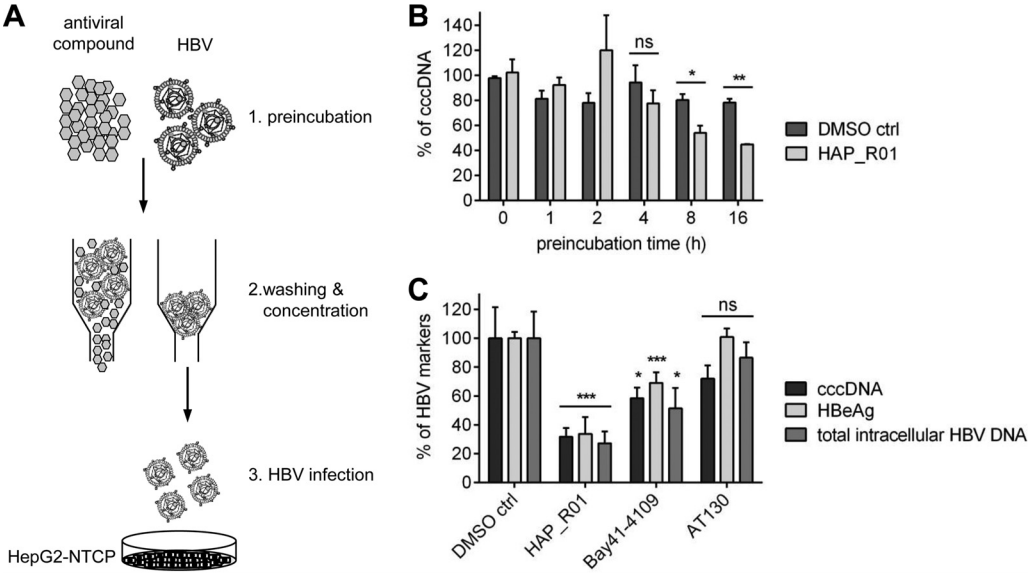

FIG 4 Effect of CpAMs on the infectivity of HBV particles. (A) An illustration showing a procedure of HAP_R01 preincubation with purified HBV particles and recovery following HBV infectivity test. HBV particles were incubated with antivirals in a reaction volume of 1 ml of Dulbecco modified Eagle medium containing penicillin-streptomycin. HBV particles were then recovered by using a Vivaspin centrifugal concentrator (100,000 MWCO; Sartorius) during which an excess amount of antivirals was washed away. (B) HBV particles were preincubated with either DMSO or HAP_R01 (5 μM) for increasing times at 37°C and recovered as depicted in panel A. HepG2-NTCP-K7 cells were infected with DMSO- or HAP_R01-preincubated HBV. cccDNA levels were analyzed by qPCR relative to control. (C) HBV particles preincubated with indicated anti-HBV compounds (5 μM each; 37°C for 16 h) were used for HBV infection similarly to panel B. At 7 dpi, intracellular viral DNA and extracellular HBeAg levels were determined by qPCR and enzyme-linked immunosorbent assay (ELISA), respectively. Student's *t* test was used (***, $P \leq 0.001$; **, $P \leq 0.01$; *, $P \leq 0.05$; ns, not significant).

the pre-S1 domain of L-HBsAg (23), or ETV. HAP_R01 inhibited cccDNA formation by >75% (Fig. 5A). Combinatorial treatment with HBIG or MyrB diminished cccDNA, HBeAg and HBsAg levels by >90% (Fig. 5A). As expected, ETV had no additive effect on cccDNA establishment, implying that the reverse transcriptase activity of HBV polymerase is not required for the conversion of rcDNA to cccDNA (24).

To model a "postexposure" use of HAP_R01, we added HAP_R01 after HBV infection and evaluated its antiviral activity. HAP_R01 reduced cccDNA, total intracellular HBV-DNA, and HBeAg levels when added 12 h p.i. for 60 h, whereas HBIG and MyrB did not have a significant antiviral effect (Fig. 5B). Similar to the treatment during infection, an additive effect on cccDNA formation was observed when cells were treated with HBIG or MyrB during HBV inoculation, but HAP_R01 was added only after HBV infection (Fig. 5C). These data indicate that HAP_R01 exerts anti-HBV activity via a distinct MOA in comparison to entry inhibitors and has the potential to prevent *de novo* cccDNA formation postexposure.

DISCUSSION

It is well known that CpAMs efficiently inhibit HBV reproduction by modulating the assembly of newly forming capsids at a late step in the virus life cycle. However, their effects on early stages of HBV infection, i.e., before cccDNA formation, are less well characterized. In this study, we showed for the first time that HAP analogue HAP_R01 physically alters capsid integrity in intact virions and early after HBV infection. It is thus able to affect HBV infectivity and to inhibit cccDNA formation during *de novo* HBV infection. This MOA was distinct from that of known entry inhibitors, allowing an additive antiviral activity during and shortly after HBV infection.

Several lines of evidence supported our finding. First, HAP_R01 treatment during establishment of infection significantly reduced cccDNA levels in HepG2-NTCP-K7 cells, in PHH, and in HepaRG cells, however, at a concentration that was 10- to 30-fold higher than the EC_{50} needed to inhibit HBV replication. This is most likely attributed to a

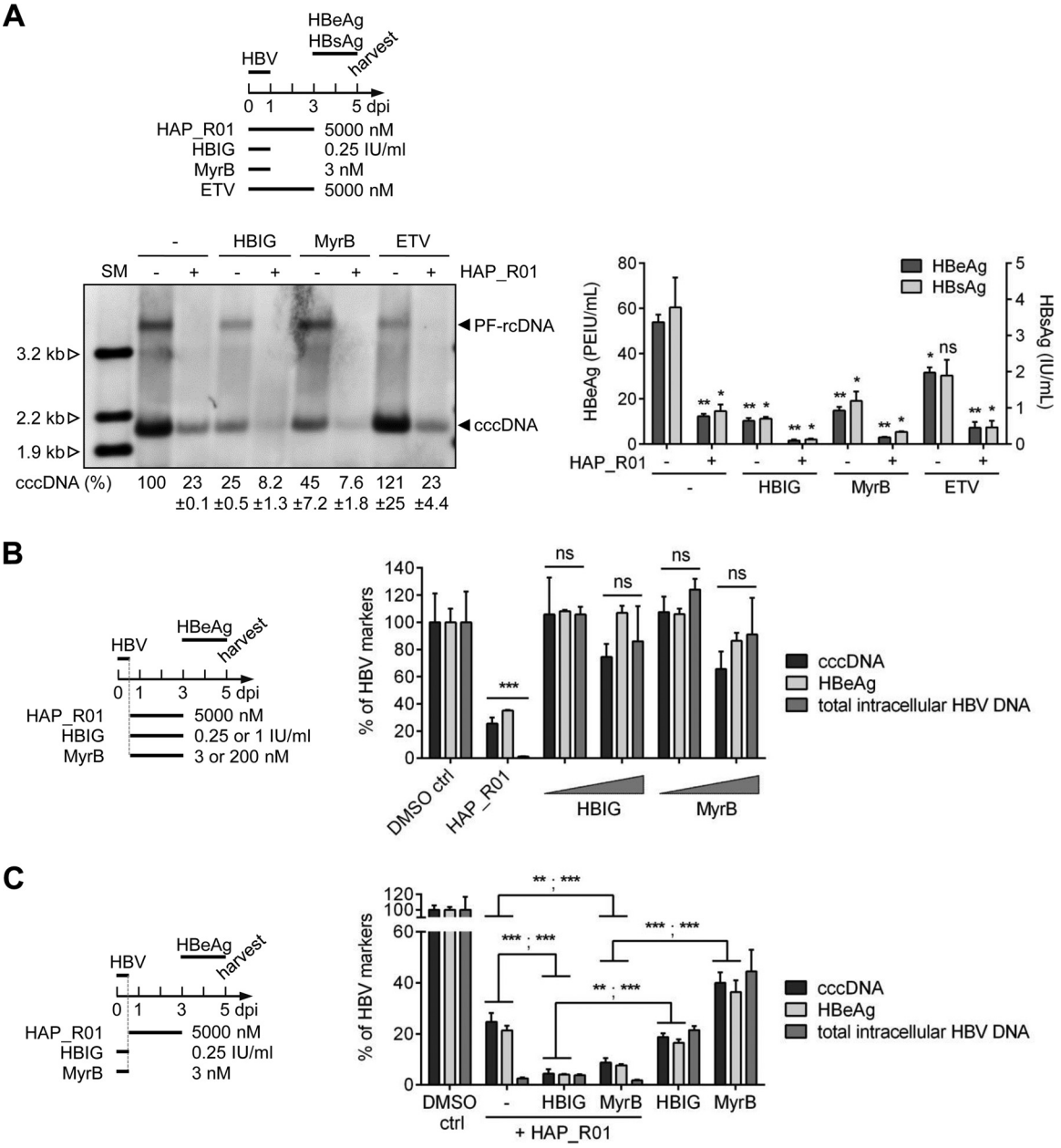

FIG 5 Evaluation of efficacy of HAP_R01 treatment in combination with entry inhibitors on cccDNA formation. (A) HepG2-NTCP-K7 cells were infected with HBV at an MOI of 500 vp/cell and treated with different anti-HBV drugs for indicated time periods either alone or in combination. At 5 dpi, cellular DNA extracted according to the Hirt method was subjected to Southern blot analysis (left). cccDNA and PF-rcDNA are denoted. cccDNA bands were quantified and shown as mean ± SD from two independent experiments. Three HBV-DNA fragments (3.2, 2.2, and 1.9 kb) serve as size markers (SM). HBsAg and HBeAg in extracellular medium were quantified by immunoassay (right). (B and C) HepG2-NTCP-K7 cells were infected at an MOI of 100 vp/cell for 12 h. During or after HBV inoculation, different anti-HBV drugs were applied either alone or in combination as indicated. cccDNA, total intracellular HBV-DNA, and HBeAg levels were analyzed by qPCR and ELISA. Student's *t* test was used (***, $P \leq 0.001$; **, $P \leq 0.01$; *, $P \leq 0.05$; ns, not significant).

reduced accessibility of HAP_R01 to assembled capsids compared to core dimers that form new capsids (15). Our preliminary data showing that HAP_R01 preferentially binds to newly translated core proteins rather than preexisting core proteins support our rationale (C. Ko and U. Protzer, unpublished results). Second, neither pretreatment of cells before HBV infection for 48 h nor HAP_R01 treatment after cccDNA establishment affected cccDNA levels, indicating a targeting of mature HBV capsids rather than a direct effect on cccDNA. Third, HAP-type CpAMs HAP_R01 and Bay41-4109 and PPA-type AT130, but not the reverse transcriptase inhibitor ETV, inhibited cccDNA forma-

tion, indicating an antiviral activity of CpAMs during early infection events. Fourth, HAP_R01 was able to change the structure and physical properties of preformed capsids, resulting in an electrophoretic mobility shift and increased sensitivity to proteinase K treatment. Last, HAP_R01 applied after treatment with entry inhibitor HBIG or MyrB resulted in a further reduction of cccDNA, indicating that HAP_R01 prevents establishment of HBV infection via a unique MOA in comparison to other entry inhibitors.

Our results are in line with recently published reports showing that selected CpAMs can prevent cccDNA synthesis (17–19). Berke et al. first reported that JNJ-632 had an effect on cccDNA formation when applied during or up to 8 h p.i. in PHH; however, they could not dissect the underlying mechanism (17). Guo et al. reported that Bay41-4109, ENAN-34017, and GLS4 inhibit cccDNA formation and provided evidence that those CpAMs can act on preformed capsids (18). Although we could confirm this effect, we did not observe contradictory effects as a consequence of CpAM action, i.e., inhibiting cccDNA synthesis during *de novo* infection versus enhancing cccDNA synthesis from intracellular amplification pathways.

In this study, we provide direct evidence that HAP_R01 can target "preformed" capsids and change their physical properties by electron microscopic and biochemical studies. Importantly, the effects of HAP_R01 on preformed capsids were confirmed upon *de novo*-infected cells. We first treated *E. coli*-expressed capsids, purified after disassembly and reassembly to remove any nonassembled core dimers, with HAP_R01. This resulted in aberrant core protein polymers, consistent with observations that HAP compounds (Bay41-4109 and a fluorophore-labeled HAP) can disrupt preassembled capsids *in vitro* (12, 25). To further investigate the effect of HAP_R01 on mature, HBV-DNA-containing capsids, we performed native agarose gel electrophoresis. Electron microscopy was not possible due to low yield and purity of mature capsids (data not shown). In native agarose gel electrophoresis, the mobility of viral capsids is primarily determined by surface charge and mass, and mobility shifts can be considered an indicator of physical or structural changes (21). We found a time- and concentration-dependent mobility shift of mature capsids under HAP_R01 treatment. Bay41-4109, another HAP-type CpAM, induced mobility shifts to a lesser degree, whereas AT130, a PPA-derivative CpAM, did not. This could reflect either differences in MOA of the distinct chemical classes or biological EC_{50} value.

Notably, HAP_R01-induced capsid alteration was confirmed in the HepG2-NTCP HBV infection model that allows detection of incoming capsids. The addition of HAP_R01 during HBV inoculation affected capsids released from purified virions after virus entry and altered their electrophoretic mobility. Trypsin treatment ensured that intracellular capsid and corresponding core protein were affected. Interestingly, we found a reduction of the amount of core protein shortly after infection upon HAP_R01 treatment that may be explained by accelerated proteasome-mediated degradation of core protein (13). However, we did not detect an induction of ISG expression, although activation of pattern recognition receptors by aberrant protein structures or by rcDNA released from capsids within the cytoplasm would be possible. This suggests that innate immune responses did not contribute to HAP_R01-mediated capsid degradation. A weak functional DNA-sensing pathway in hepatocytes (26) and the detection of HBV-DNA within the structurally altered capsids would prevent the activation of cell-intrinsic immunity.

Although all our experiments point at a structural alteration of the incoming HBV capsid upon HAP_R01 treatment, the question remains of why these structural changes result in reduced cccDNA levels. Based on dynamics of HBV capsid that could transiently dissociate and reassociate resulting from weak intersubunit interaction and alterations of tensional integrity due to HAP binding (27, 28) and the degree of structural alteration of capsids, we envision two potential mechanisms that are not mutually exclusive. First, incoming capsids could be degraded if the association of capsids and HAP_R01 is strong enough to induce severe structural changes. This option is supported by the reduced core protein levels stemming from incoming capsids. Second, altered capsids may have an impaired binding to host factors, resulting in

defects in intracellular trafficking or nuclear import. Premature disassembly of capsids or a wrong timing of viral genome release into the cytoplasm instead of nuclear targeting may account for a reduced cccDNA establishment, as proposed by Guo et al. (18). However, this seems unlikely in our experiments because the majority of HBV-DNA was still located in structurally altered capsids and resistant to DNase I treatment. The reason for this discrepancy is not clear at present, but we speculate that this may be attributable to the source or isolation methods of mature capsids or DNase treatment condition.

Interestingly, preincubation of HBV particles in the virus inoculum with HAP_R01 could also suppress the establishment of cccDNA in infected cells. This suggests that HAP_R01 targeted the capsid within HBV virions and affected their infectivity. As the viral envelope is composed of a cell-derived lipid bilayer with embedded viral envelope proteins, it seems plausible that a small molecule possessing cell membrane permeancy could pass through a viral envelope. Of note, all antiviral effects of HAP_R01 were obtained by simple addition of HAP_R01 into cell culture medium, indicating adequate cell permeancy of HAP_R01. Additionally, HAP_R01 was shown to be a moderately permeant compound in a parallel artificial membrane permeability assay (PAMPA) and a Caco-2 permeability assay (data not shown). Our finding suggests that HAP_R01 may be able not only to enter cells but even to enter into circulating infectious HBV particles in patient serum and alter their capsid structure.

Supporting a distinct MOA of HAP_R01 on cccDNA establishment, we showed an additive effect when HAP_R01 was combined with HBV entry inhibitor HBIG or MyrB. Hereby, HAP_R01 was the only drug still having an effect 12 h postexposure, i.e., after initial virus binding and uptake. A clinical situation where this may be interesting is mother-to-child transmission. However, this may be limited by the dose required. A relatively high EC_{50} (345 to 918 nM) was determined to target incoming capsids and inhibit cccDNA formation, and a dose achieving this effect *in utero* or directly after birth may not be realistic. In chronic hepatitis B patients, the effect of HAP_R01 on cccDNA formation effect will overlap the inhibitory activity on progeny virus production and thus may not become visible. Since EC_{50} alone is not predictive for the clinical outcome of anti-HIV drugs (29), further assessment of HAP_R01's performance (e.g., efficacy, toxicity, and bioavailability) in animal models supporting the full HBV life cycle and, more importantly, in clinical trials will be required to predict its superiority to other treatments and the role of HAP-resistant HBV variants.

In summary, we deciphered the antiviral effects of a novel HAP derivative, HAP_R01, possessing potent and core protein-specific anti-HBV activity. Our data highlight a dual effect of HAP_R01 on cccDNA formation by targeting incoming virions and capsids as well as on virion production by modulating capsid assembly and support further evaluation of a clinical benefit of HAP_R01.

MATERIALS AND METHODS

HBV infection. HBV (genotype D; subtype ayw) was purified from the extracellular medium of HepAD38 cells by heparin affinity chromatography and a subsequent sucrose gradient ultracentrifugation step and used as inoculum for infecting HepG2-NTCP-K7 cells as described previously (30, 31). HepG2-NTCP-K7 cells were seeded on collagen-coated plates (e.g., 1×10^6 cells for a 6-well plate and 2.5×10^5 cells for a 24-well plate), predifferentiated with 2.5% dimethyl sulfoxide (DMSO) for 2 days, and infected with HBV in the presence of 4% polyethylene glycol (PEG) 6000 for at least 16 h.

qPCR of HBV genomes. cccDNA and total intracellular HBV-DNA were analyzed after extraction of total cellular DNA using the NucleoSpin Tissue kit (Macherey-Nagel). DNA isolated from HepG2-NTCP cells was treated with T5 exonuclease (NEB) for 30 min in a 10-μl reaction volume followed by heat inactivation at 95°C for 5 min to remove non-cccDNA species (9), while DNA isolated from HepaRG cells or PHH was directly used for selective cccDNA detection as described previously (32). Target genes were normalized by two reference genes encoding prion protein (*PRNP*) and mitochondrial cytochrome *c* oxidase subunit 3 (*MT-CO3*) (9). DNA extracted from extracellular medium was used for qPCR to measure extracellular HBV-DNA contents.

Southern blot analysis of cccDNA. Protein-free, low-molecular-weight DNA species, including cccDNA, were extracted using a modified Hirt procedure (9, 33). HBV-infected cells in a 35-mm dish were lysed in 1 ml lysis buffer (50 mM Tris-HCl [pH 7.5], 150 mM NaCl, 10 mM EDTA, and 1% SDS) with gentle agitation at 37°C for 1 h. KCl was added to 500 mM, and the lysate was incubated at 4°C overnight. After centrifugation, the supernatant was subjected to phenol-chloroform extraction twice. Hirt DNA was

precipitated using isopropanol with 20 μg glycogen and subjected to Southern blot analysis with a digoxigenin-labeled HBV-specific probe (30).

Isolation and analysis of HBV capsids from hepatoma cells. HepG2-NTCP-K7-H1.3L$^-$ cells were lysed with 50 mM Tris-HCl (pH 8.0), 150 mM NaCl, 1 mM EDTA, and 1% NP-40. Obtained cell lysate was layered on top of a preformed CsCl step gradient in phosphate-buffered saline (PBS) (densities ranging from 1.10 to 1.88 g/ml; 6 steps) and centrifuged at 32,000 rpm for 16 h at 10°C in a Beckman SW32Ti rotor. Twenty-three fractions (1.5 ml each) were collected. For capsid analysis, gradient fractions 8 to 9 and 11 to 12 were pooled, washed with 10 mM Tris-HCl (pH 7.5)–150 mM NaCl–1 mM EDTA and concentrated using a centrifugal filter device (100,000-molecular-weight cutoff [MWCO]). Capsids (ca. 1 to 5 ng) were resolved on a 1.2% agarose gel, transferred onto a polyvinylidene difluoride (PVDF) membrane, and visualized using anti-HBV core antibody (Dako) (34). To analyze HBV-DNA within capsids, the membrane was incubated with denaturation buffer (0.5 N NaOH-1.5 M NaCl) for 1 min and 5 min with neutralization buffer (500 mM Tris-HCl [pH 7.0]-1.5 M NaCl). After UV-cross-linking, HBV-DNA was visualized by hybridization with a digoxigenin-labeled HBV-specific probe. For incoming capsid detection, 1×10^6 to 2×10^6 cells were treated with trypsin-EDTA for 3 min to remove cell surface-bound but not internalized HBV particles, lysed in 100 μl 1% NP-40 buffer for 15 min on ice, and centrifuged to pellet debris and nuclei. The obtained cell lysate was directly used for capsid analysis.

Transmission electron microscopy. Purified *E. coli*-expressed HBV capsids, described in the supplemental material, were absorbed onto glow-discharged carbon-coated grids. The grids were then stained with 1% (wt/vol) uranyl acetate for 10 s, washed with deionized water, and dried for 20 min. Images were acquired under an FEI 120-kV transmission electron microscope with a magnification of ×67,000.

SUPPLEMENTAL MATERIAL

Supplemental material is available online only.

SUPPLEMENTAL FILE 1, PDF file, 1 MB.

ACKNOWLEDGMENTS

We thank Stephan Urban for providing Myrcludex B and Jochen M. Wettengel, Jan-Hendrick Bockmann, and Daniela Stadler for their helpful advice. We thank Jane A. McKeating for critical reading of the manuscript.

The study was supported by the German Research Foundation (DFG) via TRR 179 (project TP14) and by the German Center for Infection Research (DZIF, projects 05.806 and 05.707) to U.P. and by the Roche Postdoc Fellowship Program to C.K.

X.Z., Z.X., and L.G. are employees of Roche R&D Center (China) Ltd. U.P. serves as an *ad hoc* advisor for Arbutus, Vir Biotechnology, Vaccitech, Gilead, Merck, Roche, and J&J.

C.K., L.G., and U.P. initiated and designed the study; C.K., R.B., X.Z., Z.X., C.B., and J.S. performed the experiments; F.W.R.V. provided key materials and contributed to the execution of the experiments; C.K. and U.P. wrote the manuscript.

REFERENCES

1. WHO. 18 July 2019. Hepatitis B, fact sheet. WHO, Geneva, Switzerland. https://www.who.int/news-room/fact-sheets/detail/hepatitis-b.
2. Schweitzer A, Horn J, Mikolajczyk RT, Krause G, Ott JJ. 2015. Estimations of worldwide prevalence of chronic hepatitis B virus infection: a systematic review of data published between 1965 and 2013. Lancet 386:1546–1555. https://doi.org/10.1016/S0140-6736(15)61412-X.
3. Lok AS, Zoulim F, Dusheiko G, Ghany MG. 2017. Hepatitis B cure: from discovery to regulatory approval. J Hepatol 67:847–861. https://doi.org/10.1016/j.jhep.2017.05.008.
4. Seeger C, Mason WS. 2015. Molecular biology of hepatitis B virus infection. Virology 479-480:672–686. https://doi.org/10.1016/j.virol.2015.02.031.
5. Hong X, Kim ES, Guo H. 2017. Epigenetic regulation of hepatitis B virus covalently closed circular DNA: implications for epigenetic therapy against chronic hepatitis B. Hepatology 66:2066–2077. https://doi.org/10.1002/hep.29479.
6. Lewellyn EB, Loeb DD. 2011. The arginine clusters of the carboxy-terminal domain of the core protein of hepatitis B virus make pleiotropic contributions to genome replication. J Virol 85:1298–1309. https://doi.org/10.1128/JVI.01957-10.
7. Tan Z, Pionek K, Unchwaniwala N, Maguire ML, Loeb DD, Zlotnick A. 2015. The interface between hepatitis B virus capsid proteins affects self-assembly, pregenomic RNA packaging, and reverse transcription. J Virol 89:3275–3284. https://doi.org/10.1128/JVI.03545-14.
8. Chu TH, Liou AT, Su PY, Wu HN, Shih C. 2014. Nucleic acid chaperone activity associated with the arginine-rich domain of human hepatitis B virus core protein. J Virol 88:2530–2543. https://doi.org/10.1128/JVI.03235-13.
9. Ko C, Chakraborty A, Chou WM, Hasreiter J, Wettengel JM, Stadler D, Bester R, Asen T, Zhang K, Wisskirchen K, McKeating JA, Ryu WS, Protzer U. 2018. Hepatitis B virus genome recycling and de novo secondary infection events maintain stable cccDNA levels. J Hepatol 69:1231–1241. https://doi.org/10.1016/j.jhep.2018.08.012.
10. Zlotnick A, Venkatakrishnan B, Tan Z, Lewellyn E, Turner W, Francis S. 2015. Core protein: a pleiotropic keystone in the HBV lifecycle. Antiviral Res 121:82–93. https://doi.org/10.1016/j.antiviral.2015.06.020.
11. Feld JJ, Colledge D, Sozzi V, Edwards R, Littlejohn M, Locarnini SA. 2007. The phenylpropenamide derivative AT-130 blocks HBV replication at the level of viral RNA packaging. Antiviral Res 76:168–177. https://doi.org/10.1016/j.antiviral.2007.06.014.
12. Stray SJ, Zlotnick A. 2006. BAY 41-4109 has multiple effects on hepatitis B virus capsid assembly. J Mol Recognit 19:542–548. https://doi.org/10.1002/jmr.801.
13. Deres K, Schroder CH, Paessens A, Goldmann S, Hacker HJ, Weber O, Kramer T, Niewohner U, Pleiss U, Stoltefuss J, Graef E, Koletzki D, Masantschek RN, Reimann A, Jaeger R, Gross R, Beckermann B, Schlemmer KH, Haebich D, Rubsamen-Waigmann H. 2003. Inhibition of hepatitis B virus replication by drug-induced depletion of nucleocapsids. Science 299:893–896. https://doi.org/10.1126/science.1077215.
14. Qiu Z, Lin X, Zhang W, Zhou M, Guo L, Kocer B, Wu G, Zhang Z, Liu H,

Shi H, Kou B, Hu T, Hu Y, Huang M, Yan SF, Xu Z, Zhou Z, Qin N, Wang YF, Ren S, Qiu H, Zhang Y, Zhang Y, Wu X, Sun K, Zhong S, Xie J, Ottaviani G, Zhou Y, Zhu L, Tian X, Shi L, Shen F, Mao Y, Zhou X, Gao L, Young JAT, Wu JZ, Yang G, Mayweg AV, Shen HC, Tang G, Zhu W. 2017. Discovery and pre-clinical characterization of third-generation 4-H heteroaryldihydropyrimidine (HAP) analogues as hepatitis B virus (HBV) capsid inhibitors. J Med Chem 60:3352–3371. https://doi.org/10.1021/acs.jmedchem.7b00083.

15. Zhou Z, Hu T, Zhou X, Wildum S, Garcia-Alcalde F, Xu Z, Wu D, Mao Y, Tian X, Zhou Y, Shen F, Zhang Z, Tang G, Najera I, Yang G, Shen HC, Young JA, Qin N. 2017. Heteroaryldihydropyrimidine (HAP) and sulfamoylbenzamide (SBA) inhibit hepatitis B virus replication by different molecular mechanisms. Sci Rep 7:42374. https://doi.org/10.1038/srep42374.
16. Yan Z, Wu D, Hu H, Zeng J, Yu X, Xu Z, Zhou Z, Zhou X, Yang G, Young JAT, Gao L. 2019. Direct inhibition of hepatitis B e antigen by core protein allosteric modulator. Hepatology 70:11–24. https://doi.org/10.1002/hep.30514.
17. Berke JM, Dehertogh P, Vergauwen K, Van Damme E, Mostmans W, Vandyck K, Pauwels F. 2017. Capsid assembly modulators have a dual mechanism of action in primary human hepatocytes infected with hepatitis B virus. Antimicrob Agents Chemother 61:e00560-17. https://doi.org/10.1128/AAC.00560-17.
18. Guo F, Zhao Q, Sheraz M, Cheng J, Qi Y, Su Q, Cuconati A, Wei L, Du Y, Li W, Chang J, Guo JT. 2017. HBV core protein allosteric modulators differentially alter cccDNA biosynthesis from de novo infection and intracellular amplification pathways. PLoS Pathog 13:e1006658. https://doi.org/10.1371/journal.ppat.1006658.
19. Lahlali T, Berke JM, Vergauwen K, Foca A, Vandyck K, Pauwels F, Zoulim F, Durantel D. 2018. Novel potent capsid assembly modulators regulate multiple steps of the hepatitis B virus life cycle. Antimicrob Agents Chemother 62:e00835-18. https://doi.org/10.1128/AAC.00835-18.
20. Cui X, Ludgate L, Ning X, Hu J. 2013. Maturation-associated destabilization of hepatitis B virus nucleocapsid. J Virol 87:11494–11503. https://doi.org/10.1128/JVI.01912-13.
21. Wu S, Luo Y, Viswanathan U, Kulp J, Cheng J, Hu Z, Xu Q, Zhou Y, Gong GZ, Chang J, Li Y, Guo JT. 2018. CpAMs induce assembly of HBV capsids with altered electrophoresis mobility: implications for mechanism of inhibiting pgRNA packaging. Antiviral Res 159:1–12. https://doi.org/10.1016/j.antiviral.2018.09.001.
22. Rabe B, Delaleau M, Bischof A, Foss M, Sominskaya I, Pumpens P, Cazenave C, Castroviejo M, Kann M. 2009. Nuclear entry of hepatitis B virus capsids involves disintegration to protein dimers followed by nuclear reassociation to capsids. PLoS Pathog 5:e1000563. https://doi.org/10.1371/journal.ppat.1000563.
23. Petersen J, Dandri M, Mier W, Lutgehetmann M, Volz T, von Weizsacker F, Haberkorn U, Fischer L, Pollok JM, Erbes B, Seitz S, Urban S. 2008. Prevention of hepatitis B virus infection in vivo by entry inhibitors derived from the large envelope protein. Nat Biotechnol 26:335–341. https://doi.org/10.1038/nbt1389.
24. Qi Y, Gao Z, Xu G, Peng B, Liu C, Yan H, Yao Q, Sun G, Liu Y, Tang D, Song Z, He W, Sun Y, Guo JT, Li W. 2016. DNA polymerase kappa is a key cellular factor for the formation of covalently closed circular DNA of hepatitis B virus. PLoS Pathog 12:e1005893. https://doi.org/10.1371/journal.ppat.1005893.
25. Schlicksup CJ, Wang JC, Francis S, Venkatakrishnan B, Turner WW, VanNieuwenhze M, Zlotnick A. 2018. Hepatitis B virus core protein allosteric modulators can distort and disrupt intact capsids. Elife 7:e31473. https://doi.org/10.7554/eLife.31473.
26. Thomsen MK, Nandakumar R, Stadler D, Malo A, Valls RM, Wang F, Reinert LS, Dagnaes-Hansen F, Hollensen AK, Mikkelsen JG, Protzer U, Paludan SR. 2016. Lack of immunological DNA sensing in hepatocytes facilitates hepatitis B virus infection. Hepatology 64:746–759. https://doi.org/10.1002/hep.28685.
27. Hadden JA, Perilla JR, Schlicksup CJ, Venkatakrishnan B, Zlotnick A, Schulten K. 2018. All-atom molecular dynamics of the HBV capsid reveals insights into biological function and cryo-EM resolution limits. Elife 7:e32478. https://doi.org/10.7554/eLife.32478.
28. Ceres P, Zlotnick A. 2002. Weak protein-protein interactions are sufficient to drive assembly of hepatitis B virus capsids. Biochemistry 41:11525–11531. https://doi.org/10.1021/bi0261645.
29. Shen L, Peterson S, Sedaghat AR, McMahon MA, Callender M, Zhang H, Zhou Y, Pitt E, Anderson KS, Acosta EP, Siliciano RF. 2008. Dose-response curve slope sets class-specific limits on inhibitory potential of anti-HIV drugs. Nat Med 14:762–766. https://doi.org/10.1038/nm1777.
30. Burwitz BJ, Wettengel JM, Muck-Hausl MA, Ringelhan M, Ko C, Festag MM, Hammond KB, Northrup M, Bimber BN, Jacob T, Reed JS, Norris R, Park B, Moller-Tank S, Esser K, Greene JM, Wu HL, Abdulhaqq S, Webb G, Sutton WF, Klug A, Swanson T, Legasse AW, Vu TQ, Asokan A, Haigwood NL, Protzer U, Sacha JB. 2017. Hepatocytic expression of human sodium-taurocholate cotransporting polypeptide enables hepatitis B virus infection of macaques. Nat Commun 8:2146. https://doi.org/10.1038/s41467-017-01953-y.
31. Seitz S, Iancu C, Volz T, Mier W, Dandri M, Urban S, Bartenschlager R. 2016. A slow maturation process renders hepatitis B virus infectious. Cell Host Microbe 20:25–35. https://doi.org/10.1016/j.chom.2016.05.013.
32. Xia Y, Stadler D, Ko C, Protzer U. 2017. Analyses of HBV cccDNA quantification and modification. Methods Mol Biol 1540:59–72. https://doi.org/10.1007/978-1-4939-6700-1_6.
33. Yan H, Zhong G, Xu G, He W, Jing Z, Gao Z, Huang Y, Qi Y, Peng B, Wang H, Fu L, Song M, Chen P, Gao W, Ren B, Sun Y, Cai T, Feng X, Sui J, Li W. 2012. Sodium taurocholate cotransporting polypeptide is a functional receptor for human hepatitis B and D virus. Elife 1:e00049. https://doi.org/10.7554/eLife.00049.
34. Ko C, Lee S, Windisch MP, Ryu WS. 2014. DDX3 DEAD-box RNA helicase is a host factor that restricts hepatitis B virus replication at the transcriptional level. J Virol 88:13689–13698. https://doi.org/10.1128/JVI.02035-14.